International Journal of Agriculture and Environmental Research

ISSN: 2455-6939

Volume: 06, Issue: 02 "March-April 2020"

BIOCHAR PARTICLE SIZE EFFECT ON SORPTION OF PLANT NUTRIENTS

[1*]Tang Tze Piew, [1]Rosenani Abu Bakar, [2]Mohamad Amran b. Mohd Salleh

[1]Department of Land Management, Faculty of Agriculture, Universiti Putra Malaysia, Serdang, Selangor, Malaysia

[2]Department of Chemical and Environmental Engineering, Faculty of Engineering, Universiti Putra Malaysia, Serdang, Selangor, Malaysia

*Corresponding author

DOI: 10.46609/IJAER.2020.v06i02.009 **URL:** https://doi.org/10.46609/IJAER.2020.v06i02.009

ABSTRACT

The pyrolysis of biomass into biochar can served as nutrient absorbent in soil to counter excessive leaching problem commonly faced by agriculture sector in tropical region. The present study investigated the particle size of biochar on the sorption of ammonium N (NH_4^+-N), nitrate N (NO_3^--N), phosphate P (PO_4^{3-}), and iron (Fe^{3+}). Four biochars were produced from oil palm empty fruit bunch (EFB), oil palm kernel shell (KRN), rice husk (RH), and bamboo (BMB), which sieved into two groups with particle size of 1-2 mm and <0.3 mm. Biochar physical and chemical properties were determined. The ability of biochars to adsorb NH_4^+ followed: BMB > RH > EFB while no sorption was observed in KRN. The sorption characteristics of NH_4^+ were well fitted to the Freundlich isotherm model. Overall sorption of NO_3^- favours fine particle and were well-fitted into Langmuir model followed the maximum sorption capacity of: BMB > EFB > KRN > RH. Sorption of PO_4^{3-} on the other hand performed poorly among all tested biochar while sorption of Fe^{3+} were generally favourable in fine particle and best-fitted in Langmuir model with the maximum sorption capacity followed: EFB > RH > KRN > BMB.

Keywords: Biochar, Nutrient Sorption, Particle Size

INTRODUCTION

One of the important environmental management aspect is the recovery of nutrient in soil as they are contributors to eutrophication (Rittmann *et al*., 2011; Zeng *et al*., 2013; Wang *et al*., 2015), which are usually found in several wastewaters at varying concentrations (Ye *et al*., 2010; Song

ISSN: 2455-6939

Volume: 06, Issue: 02 "March-April 2020"

et al., 2011; Cai *et al*., 2013). Ammonium accounted for a great portion of soluble nitrogen in animal manure and is likely to be adsorbed on negatively-charged sites or between clay interlayers in soils. As the release of ammonium takes place, nitrification occurs due to the present of nitrifying bacteria, converting ammonium into nitrate under aerobic conditions which eventually leached to nearby groundwater (Fernando *et al*., 2005). Another essential nutrient in plant i.e. phosphate, in which the recovery from soil is also important as there are growing concerns about its future availability (Rittmann *et al*., 2011). A number of nutrient adsorbents have therefore been considered including chars obtained from thermal treatment of organic biomass in an oxygen-limited atmosphere. Biochar is considered as a potential applicable material to mitigate nutrient leaching, since a few studies have indicated that it can affect availability and cycling of nutrient in soil (Ding *et al*., 2010; Laird *et al*., 2010; Hollister *et al*., 2013). However, confounding results have been reported with regard to the effect of biochar application on nutrient leaching. While some findings observed a reduction of nutrient such as ammonium and total N leaching in top soil up to 15% after the addition of biochar (Ding *et al*., 2010; Laird *et al*., 2010), other research oppositely found a limited to no sorption ability of biochar towards nutrient (Yao *et al*., 2012; Hollister *et al*., 2013), especially towards nitrate and phosphate.

The temperature during pyrolysis process and the types of feedstock being used determines the molecular structure and pores size distribution of biochar, which changes the sorption characteristics on biochar (Keiluweit *et al*., 2010; Ahmad *et al*., 2012). Finding also suggests that the type of feedstock resulting in different magnitudes of surface area, pores and functional groups in biochar (Sohi *et al*., 2010), and all these variables affect sorption characteristics of biochars. Regardless of the temperature of pyrolysis, two biochar produced under same temperature resulted larger specific surface area and porosity in poultry-litter biochar than wheat-straw biochar (Sun *et al*., 2011). High pyrolysis temperature generally leads to greater specific surface area and aromaticity of biochar (Ahmad *et al*., 2012).

While various findings mainly highlight on the factors such as feedstock and pyrolysis temperature (Yao *et al*., 2012; Hollister *et al*., 2013; Gai *et al*., 2014; Takaya, *et al*., 2016) effects towards the sorption behaviours of biochar on nutrients, Qin *et al*. (2012) reported the effect of physical biochar particle size on cadmium ion sorption. However, evaluation of such parameter remains scarce and insufficient to provide insight in understanding of biochar sorption behaviours.

The objective of this work was therefore to evaluate nutrient sorption behaviour on biochar at two different particle sizes.

MATERIALS AND METHODS

ISSN: 2455-6939

Volume: 06, Issue: 02 "March-April 2020"

Biochar production and characterisation

Biochars produced from four different feedstock were used in this experiment: oil palm empty fruit bunch (EFB), oil palm kernel shell (KRN), rice husk (RH), and bamboo (BMB). EFB biochar was produced from a trial biochar carbonator plant manufactured by Nasmech Technology Sdn. Bhd., Selangor. The temperature of production was around 300 - 350°C in a rotary drum design. KRN biochar was produced at Universiti Putra Malaysia (UPM) using a simple drum kiln. RH biochar was produced using a laboratory furnace with temperature set to 350°C and retention of eight hours. BMB biochar was produced using a small scale trial carbonator designed by Institute of Advance Technology (ITMA), UPM. Temperature of production for BMB biochar was 350 - 400°C.

Proximate analysis of different biochar samples was conducted according to the Standard Test Method for Chemical Analysis of Wood Charcoal (ASTM D1762 – 84, 2007) as recommended by the International Biochar Initiative (IBI). Biochar-to-distilled water mixture at 1:20 ratio for each samples were shaken and allowed to stand for 24 h before pH and electrical conductivity (EC) measurements were recorded. Total carbon of samples was measured using LECO Carbon Analyser from Department of Land Management, Faculty of Agriculture, UPM. Total nitrogen was done according to Kjeldhal Method (Bremner, 1960). The selected properties of biochar were as summarised in Table 1.

Table 1: Selected properties of biochar samples.

	EFB	RH	KRN	BMB
pH	8.0 c	4.6 d	10.2 a	9.6 b
EC (ms cm^{-1})	2.5 a	0.4 b	1.0 b	0.8 b
Moisture content	13.7 a	5.2 b	12.2 a	7.4 b
Volatile matter, %	41.2 a	26.7 b	11.8 c	28.0 b
Non-volatile matter, %	42.6 b	41.0 b	14.1 c	63.4 a
Ash, %	16.2 c	32.0 b	74.0 a	7.7 c
Total carbon, %	57.05 b	45.94 c	20.06 d	74.56 a
Total nitrogen, %	0.69 a	0.39 b	0.07 d	0.27 c

Note: Moisture content in %, expressed as fresh weight basis; volatile matter, non-volatile matter, ash, total carbon, and total nitrogen are expressed as dry weight basis in %.

Samples preparation

In this study, each biochar samples were sieved grouped into particle size of 1 – 2 mm (Coarse) and < 0.3 mm (Fine) and pre-washed to remove any dissolvable nutrients that could potentially interferes with the experiment (Fidel et al., 2013). The sieved biochar samples were pre-washed

ISSN: 2455-6939

Volume: 06, Issue: 02 "March-April 2020"

once with diluted hydrochloric acid (HCl) at 0.5 M, at the ratio of 1:50 biochar/solution for 24 h. The subsequent washing was done with distilled water for the next six consecutive days to achieve final water extracts with electrical conductivity below 30 µS cm^{-1}. Washed samples were dried in an oven at 60℃ prior to nutrient sorption experiment. The surface area, pore volume, and pore size of each biochars were determined using Brunauer–Emmett–Teller (BET) adsorption method with nitrogen gas.

Sorption of nutrient

Four nutrients of were included in this sorption experiment, i.e. ammonium N (NH_4^+), nitrate N (NO_3^-), and phosphate P (PO_4^{3-}) as macronutrients and iron (Fe^{3+}) as micronutrient. The sieved biochar samples were weighed to 0.2 g ±0.0005 in each 50 mL centrifuge tubes followed by addition of 20 mL of nutrient solution containing 0.01 M $CaCl_2$ and their respective nutrient ions of different concentration in triplicate. Each nutrient with five varying concentrations were used in this study. Concentration of ammonium was ranging from 2 to 10 mg L^{-1}; nitrate at the range between 4 to 20 mg L^{-1}; phosphate at the range between 4 to 12 mg L^{-1}; while iron at the range between 2 to 20 mg L^{-1}. The mixtures were shaken using orbital shaker for 20 hours at room temperature and let to settle down for an hour. Samples were filtered using syringe filter for analysis. The filtrates were then analysed using UV-Vis spectrophotometer (Multiskan GO Microplate Spectrophotometer, Thermo Fisher Scientific). Concentration of NH_4^+ was analysed according to indophenol blue method (Koroleff, 1976); concentration of NO_3^- was analysed according to brucine colorimetric method (EPA 1971, Method 352.1); concentration of PO_4^{3-} was analysed according to molybdenum blue method (Murphy and Riley, 1962); and concentration of Fe^{3+} was analysed using modified o-phenanthroline method (Demirhan and Tuncel Elmali, 2003) by using 1% ascorbic acid as reducing reagent in replacement of hydroquinone.

The amount of nutrient adsorbed per unit mass of biochar was calculated as:

$$Q_e = \frac{(C_0 - C_e)V}{M}$$

where Q_e is the amount of nutrient adsorbed by biochar (mg g^{-1}) at equilibrium; C_0 and C_e are the nutrient concentration in the initial and equilibrium solution (mg L^{-1}), respectively; V is the volume of the aqueous solution (L) and M is the mass of biochar (g).

The nutrient sorption data were fitted into linear Freundlich and Langmuir models which are the most frequently used models for describing sorption isotherms. The Freundlich isotherm model (Freundlich, 1906) is expressed as:

$$Q_e = K_F \cdot C_e^{\frac{1}{n}}$$

ISSN: 2455-6939

Volume: 06, Issue: 02 "March-April 2020"

and linearised into:

$$\ln Q_e = \frac{1}{n} \cdot \ln C_e + \ln K_F$$

where, Q_e is mass of nutrient adsorbed per mass of biochar (mg g^{-1}) at equilibrium C_e is equilibrium concentration (mg L^{-1}) of nutrient in solution; K_F and 1/n are experimentally derived constants.

The Langmuir isotherm model (Langmuir, 1916), which assumes homogeneous monolayer surface sorption, can be written as:

$$Q_e = \frac{Q_{max} K_L C_e}{1 + K_L C_e}$$

and linearised into:

$$\frac{C_e}{Q_e} = \frac{1}{Q_{max}} \cdot C_e + \frac{1}{Q_{max} K_L}$$

where, Qmax is maximum sorption capacity of biochar (mg g-1), and KL refers to Langmuir constants related to adsorption capacity and adsorption rate. When Ce/Qe is plotted against Ce, a straight line with a slope of $\frac{1}{Q_{max}}$ and an intercept of $\frac{1}{Q_{max} K_L}$ is obtained.

RESULTS AND DISCUSSION

BET surface area, pore volume, and pore size

BET surface area, pore volume, and pore size of the different biochars are presented in Table 2. The BET surface area and pore volume of the biochars are generally greater in coarse particle compared to its fine counterpart. The surface area of the biochars ranged between 43.4 – 5.12 $m^2 g^{-1}$. Particle size within the range of 1.0 – 2.0 mm for bamboo biochar shows highest BET surface area at 43.4 $m^2 g^{-1}$ followed by rice husk biochar at 41.75 $m^2 g^{-1}$, EFB at 12.91 $m^2 g^{-1}$, and lastly kernel shell biochar at 11.54 $m^2 g^{-1}$. Grinding down the biochar particles to below 0.3 mm observed reduction of BET surface area to a certain extend. Finer EFB biochar was 11.61 $m^2 g^{-1}$, a reduction of 10.1% in BET surface area at as the particle ground down; kernel shell biochar shows greater reduction up to 55.7%, at 5.12 $m^2 g^{-1}$; finer bamboo biochar shows greatest reduction in BET surface area at 17.33 $m^2 g^{-1}$, accounted 60.1%. Such observation was rather unusual as surface area are generally expected to increase with the

ISSN: 2455-6939

Volume: 06, Issue: 02 "March-April 2020"

decrease of particle size. However, similar situation was also reported by Jaafar *et al*. (2015) where surface area of biochar may not correlate with particle size. The reason for this observation is not properly understood and require in-depth investigation in the future.

Table 2: BET surface area, pore volume, and pore size of biochar samples.

Biochar	Particle Size	BET Surface $m^2\ g^{-1}$	Pore Volume $cm^3\ g^{-1}$	Pore Size Å
EFB	Fine	11.61	0.101	348.93
	Coarse	12.91	0.117	268.64
KRN	Fine	5.12	0.125	977.01
	Coarse	11.55	0.147	510.54
BMB	Fine	17.33	0.103	268.64
	Coarse	43.40	0.144	132.81
RH	Coarse	41.75	0.194	186.09

Coarse: 1 – 2 mm; Fine: < 0.3 mm.

Sorption of ammonium (NH_4^+)

The sorption of NH_4^+ - N to EFB, rice husk, kernel shell, and bamboo biochars were presented in Figure 1. From the figures, the affinity of sorption on NH_4^+ - N towards EFB and rice husk biochars were relatively low at low concentration, which later increases as the concentration of sorbate increases. Sorption of NH_4^+ - N was higher for coarse particle in EFB and rice husk biochar while very similar trend was observed in bamboo biochar in both sizes. However, kernel shell biochar do not exhibit any affinity to NH_4^+ - N at all concentration. Table 3 shows the constants of Freundlich and Langmuir sorption models derived from the linearising of the results at equilibrium. The results showed that the sorption of NH_4^+ - N fitted best in Freundlich model, giving higher coefficient of determination (R^2) over Langmuir model. The fitting of Freundlich model suggests the sorption sites on the surface of biochar were heterogeneous and not in monolayer formation. The values of n below 1 in EFB and rice husk biochars of both sizes suggest strong affinity of ammonium ions toward the particles of biochar as the increase of solute concentration. On the other hand, the n > 1 in bamboo biochar of both sizes suggest that the affinity of ammonium sorption onto biochar particles was gradually decreases with the

ISSN: 2455-6939

Volume: 06, Issue: 02 "March-April 2020"

increase of concentration. The sorption affinity of ammonium on biochars were as following order: EFB > rice husk > bamboo.

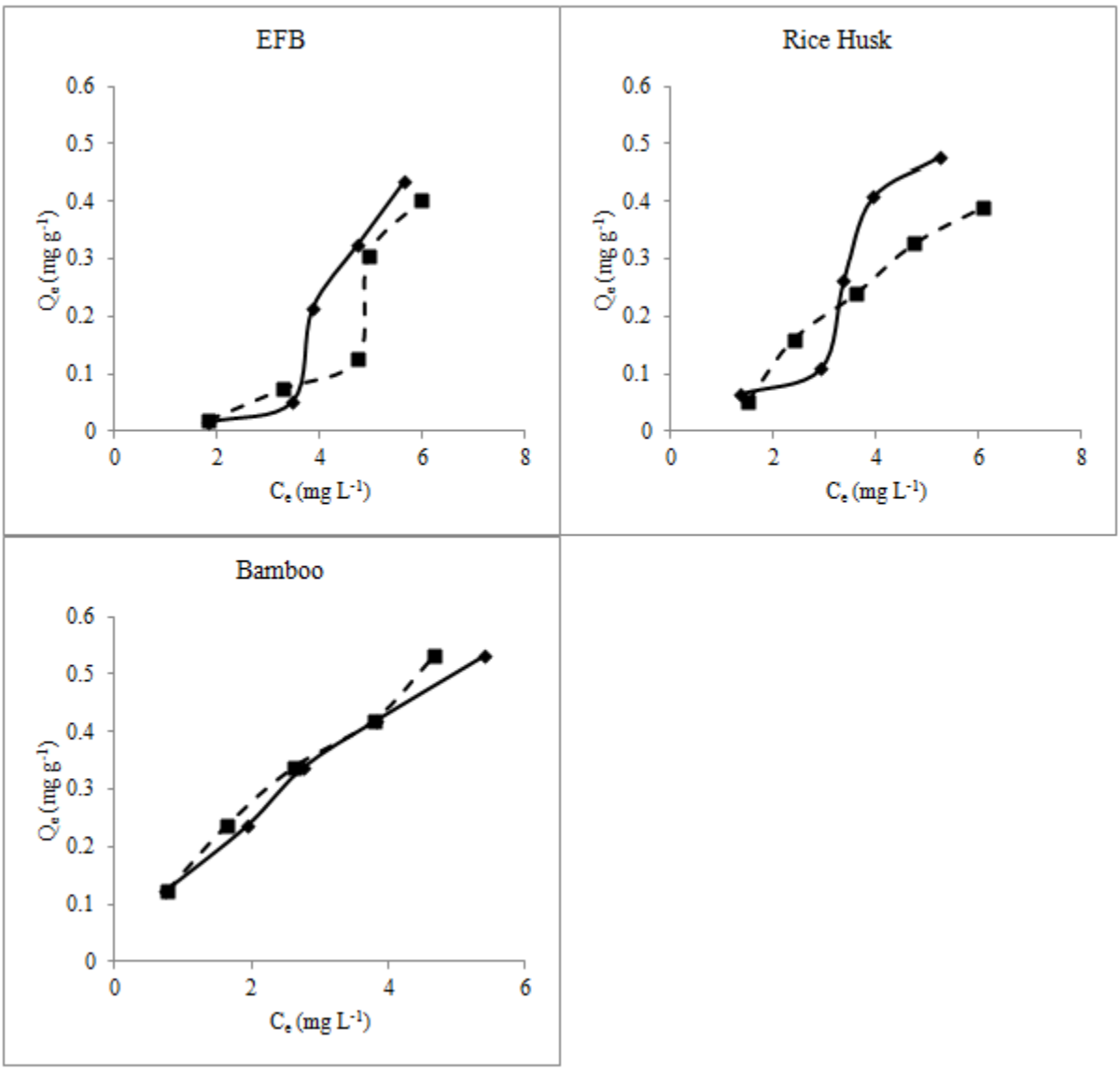

Figure 1: Sorption of NH_4^+ - N in EFB, rice husk, kernel shell, and bamboo biochars. Broken lines: fine; continuous line: coarse.

Note: Kernel shell biochar observed no sorption of NH_4^+-N in this experiment, no sorption regression was developed.

ISSN: 2455-6939

Volume: 06, Issue: 02 "March-April 2020"

Table 3: Regression parameters of isotherm for expressing sorption of NH_4^+-N to EFB, rice husk, kernel shell, and bamboo biochars at two different particle sizes.

		Freundlich			Langmuir		
		K_F	n	R^2	K_L	Q_{max}	R^2
EFB	Coarse	0.0023	0.3284	0.9106	-0.1801	-0.0369	0.83
	Fine	0.0036	0.3867	0.947	-0.1603	-0.0484	0.8745
RH	Coarse	0.0355	0.6378	0.8553	-0.1231	-0.2957	0.43
	Fine	0.0351	0.7030	0.9408	-0.0880	-0.4269	0.4151
KRN	Coarse	-	-	-	-	-	-
	Fine	-	-	-	-	-	-
BMB	Coarse	0.1516	1.2424	0.9953	0.1781	0.9523	0.8054
	Fine	0.1487	1.4302	0.9691	0.1143	1.4669	0.9201

Note: Kernel shell biochar observed no sorption of NH_4^+-N in this experiment, no sorption regression was developed.

Sorption of nitrate (NO_3^-)

All biochars exhibit certain degree of sorption to NO_3^- - N as shown in Figure 2. The sorption of NO_3^- - N has gradually increase as the concentration solution rises. The sorption data from all biochars were best fitted into Langmuir model as presented in Table 4. In general, the Q_{max} values showed higher maximum sorption capacity for fine compared to coarse particles in rice husk, kernel shell, and bamboo biochars while was reversed in EFB biochar. The sorption capacity for nitrate at maximum of coarse EFB biochar was 28.5% higher than fine particles, at 0.53 mg g^{-1}. On the other hand, the maximum sorption capacity of rice husk biochar was increased by 77.1%, at 0.68 mg g^{-1} in fine particle compared to 0.38 mg g^{-1} in coarse particle. Similarly, to rice husk biochar, the maximum sorption capacity of fine particles of kernel shell and bamboo biochars observed 17.8% and 38.3% increment, respectively as compared to their coarse counterpart. Overall maximum sorption capacity, bamboo biochar recorded highest at 0.72 and 1.00 mg g^{-1} in fine and coarse particles, respectively. Such finding on positive sorption

ISSN: 2455-6939

Volume: 06, Issue: 02 "March-April 2020"

of nitrate on biochars was reported by Shen et al. (2013) in bamboo biochar of coarser particle size. Kameyama et al. (2012) also reported the improved retention of nitrate in soil treated with sugarcane bagasse-derived biochar. They also speculate particle size as a contributing factor behind the sorption kinetics of nitrate.

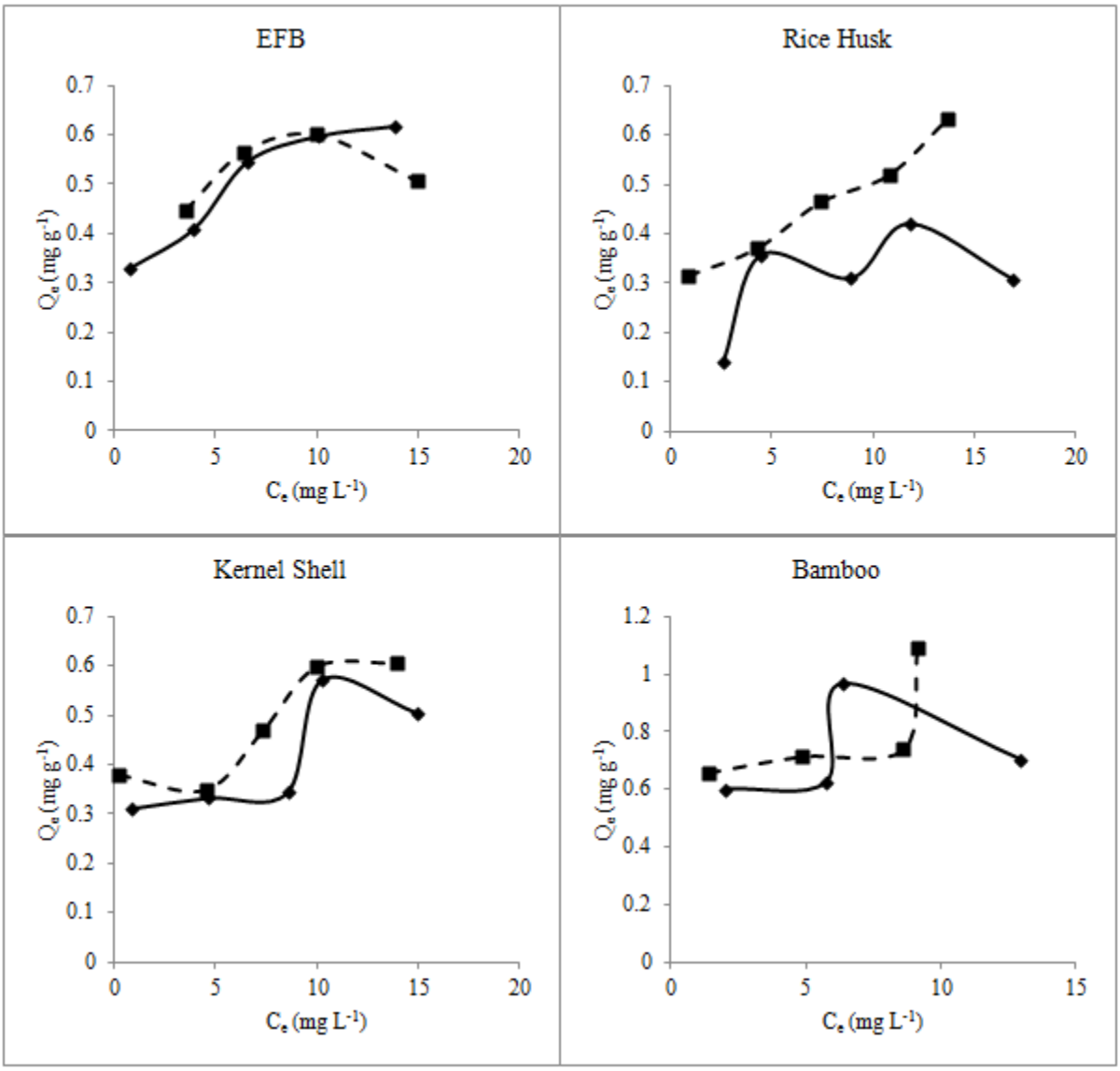

Figure 2: Sorption of NO_3^- - N in EFB, rice husk, kernel shell, and bamboo biochar. Broken lines: fine; continuous line: coarse.

ISSN: 2455-6939

Volume: 06, Issue: 02 "March-April 2020"

Table 4: Regression parameters of isotherm for expressing sorption of NO_3^--N to EFB, rice husk, kernel shell, and bamboo biochars at two different particle sizes.

		Freundlich			Langmuir		
		K_F	n	R^2	K_L	Q_{max}	R^2
EFB	Coarse	0.3401	4.4092	0.931	0.6473	0.6793	0.9838
	Fine	0.4244	9.3458	0.26	-10.954	0.5286	0.968
RH	Coarse	0.1343	2.5846	0.4824	0.5023	0.3837	0.8541
	Fine	0.3075	4.3917	0.8575	0.4112	0.6793	0.9353
KRN	Coarse	0.2953	5.6466	0.5153	0.4621	0.5616	0.8554
	Fine	0.4107	10.331	0.4304	0.5280	0.6613	0.917
BMB	Coarse	0.5865	8.9286	0.1625	69.185	0.7227	0.945
	Fine	0.5955	5.7307	0.4475	0.8013	0.9998	0.8296

Sorption of phosphate (PO_4^{3-})

The sorption of PO_4^{3-} - P on each biochars were presented in Figure 3. There were certain degree of PO_4^{3-} - P sorption seen in EFB and kernel shell biochar for both particle sizes. However, there were relatively low to no sorption observed in rice husk and bamboo biochar at coarse particle fraction. The sorption data fitted into Freundlich and Langmuir models presented in Table 5 shows that mostly were well fitted in Langmuir with relatively high R^2. Q_{max} values suggested that the maximum sorption capacity of PO_4^{3-} - P in fine EFB particle was 0.2047 mg g^{-1}, and 0.0148 and 0.0108 mg g^{-1} as in kernel shell biochar of fine and coarse particle, respectively.

ISSN: 2455-6939

Volume: 06, Issue: 02 "March-April 2020"

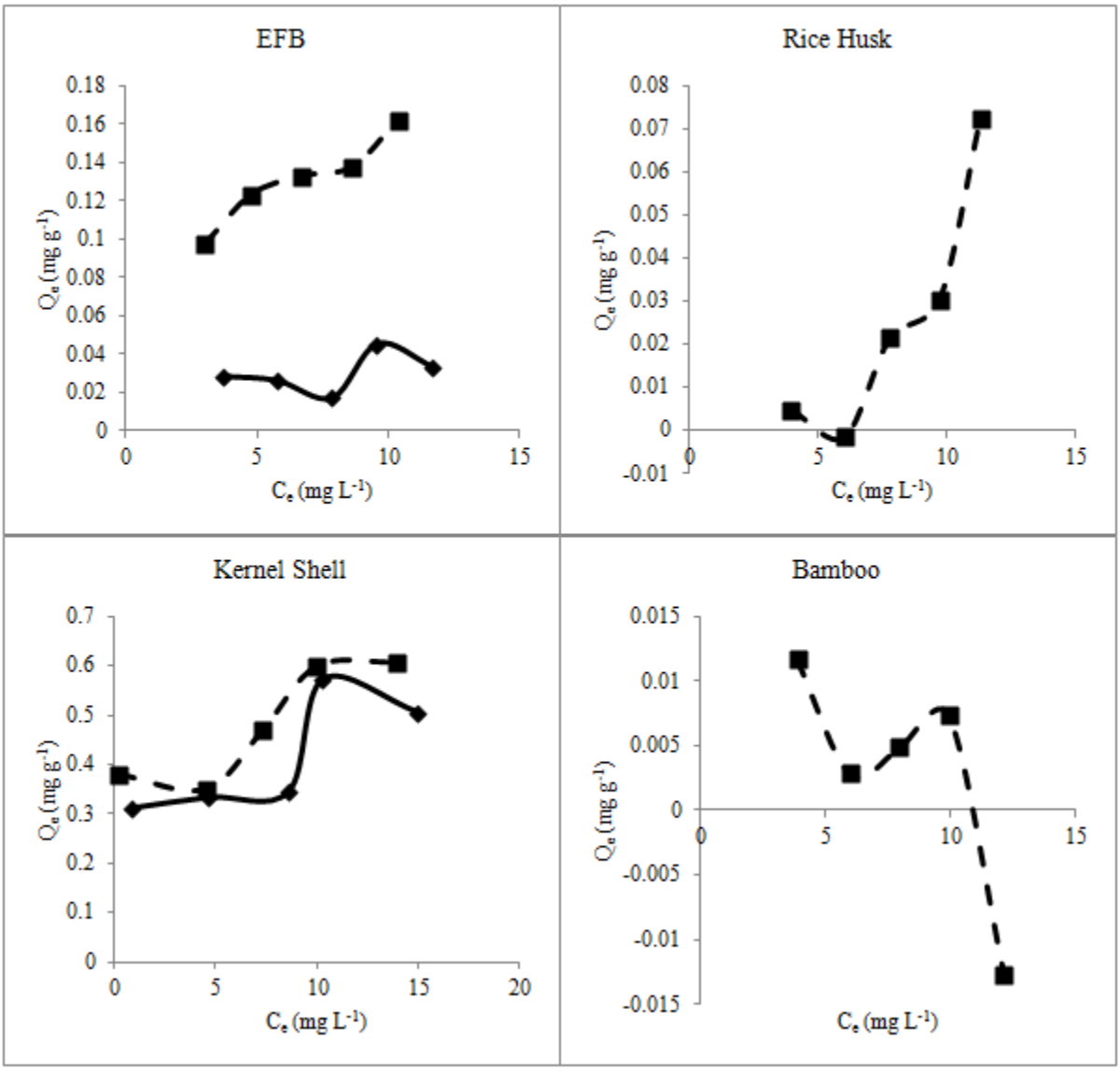

Figure 3: Sorption of PO_4^{3-} - P in EFB, rice husk, kernel shell, and bamboo biochar. Broken lines: fine; continuous line: coarse.

Note: Rice husk and bamboo biochar at coarse particle observed relatively low to no sorption of PO_4^{3-}-P in this experiment, no sorption regression was developed.

ISSN: 2455-6939

Volume: 06, Issue: 02 "March-April 2020"

Table 5: Regression parameters of isotherm for expressing adsorption of PO_4^{3-}-P to EFB, rice husk, kernel shell, and bamboo biochars at two different particle sizes.

		Freundlich			Langmuir		
		K_F	n	R^2	K_L	Q_{max}	R^2
EFB	Coarse	0.0181	4.3783	0.0833	0.2352	0.0433	0.3051
	Fine	0.0665	2.7435	0.946	0.2924	0.2047	0.966
RH	Coarse	-	-	-	-	-	-
	Fine	0.0002	0.4103	0.9668	-0.0786	-0.0107	0.9515
KRN	Coarse	0.0262	-6.3654	0.2049	-0.8096	0.0148	0.966
	Fine	0.0337	-3.8595	0.1366	-0.4054	0.0108	0.9862
BMB	Coarse	-	-	-	-	-	-
	Fine	0.0147	-2.0572	0.1097	0.3262	0.0074	0.2254

Note: Rice husk and bamboo biochar at coarse particle observed relatively low to no sorption of PO_4^{3-}-P in this experiment, no sorption regression was developed.

Sorption of Iron (Fe^{3+})

Iron (III) ion was used as an alternative cation to study the sorption on biochars with both sizes (Figure 4). All three biochars namely EFB, rice husk, and kernel shell biochar consistently showed higher sorption of Fe^{3+} at equilibrium in fine particle size while bamboo biochar shows higher sorption in coarse particle size. The results from the experiment were linearly fitted into Freundlich and Langmuir models to obtain the constant values as shown in Table 6. The overall results from all biochar were well-fitted into Langmuir isotherm model with relatively higher R^2 value than Freundlich. The fitting suggested that the sorption of Fe^{3+} on biochar was in monolayer formation. This is commonly recognised that the negatively charges (Mukherjee et al, 2011) on biochar surface served as active sites that attracts the sorption of positively charged Fe^{3+}. Based on the Q_{max} values, it clearly shows that the maximum sorption capacity of all biochars in fine particle were higher than their respective coarse fraction. The maximum sorption capacity of Fe^{3+} was highest in fine EFB biochar, projected at 0.47 mg g^{-1}, followed by a slight difference at 0.4 mg g^{-1} in coarse particle. Bamboo biochar on the other hand recorded lowest sorption capacity at 0.018 and 0.007 mg g^{-1} in its fine and coarse particles, respectively. From the figure also suggests the gradual decrease of sorption of Fe^{3+} as the concentration increase.

ISSN: 2455-6939

Volume: 06, Issue: 02 "March-April 2020"

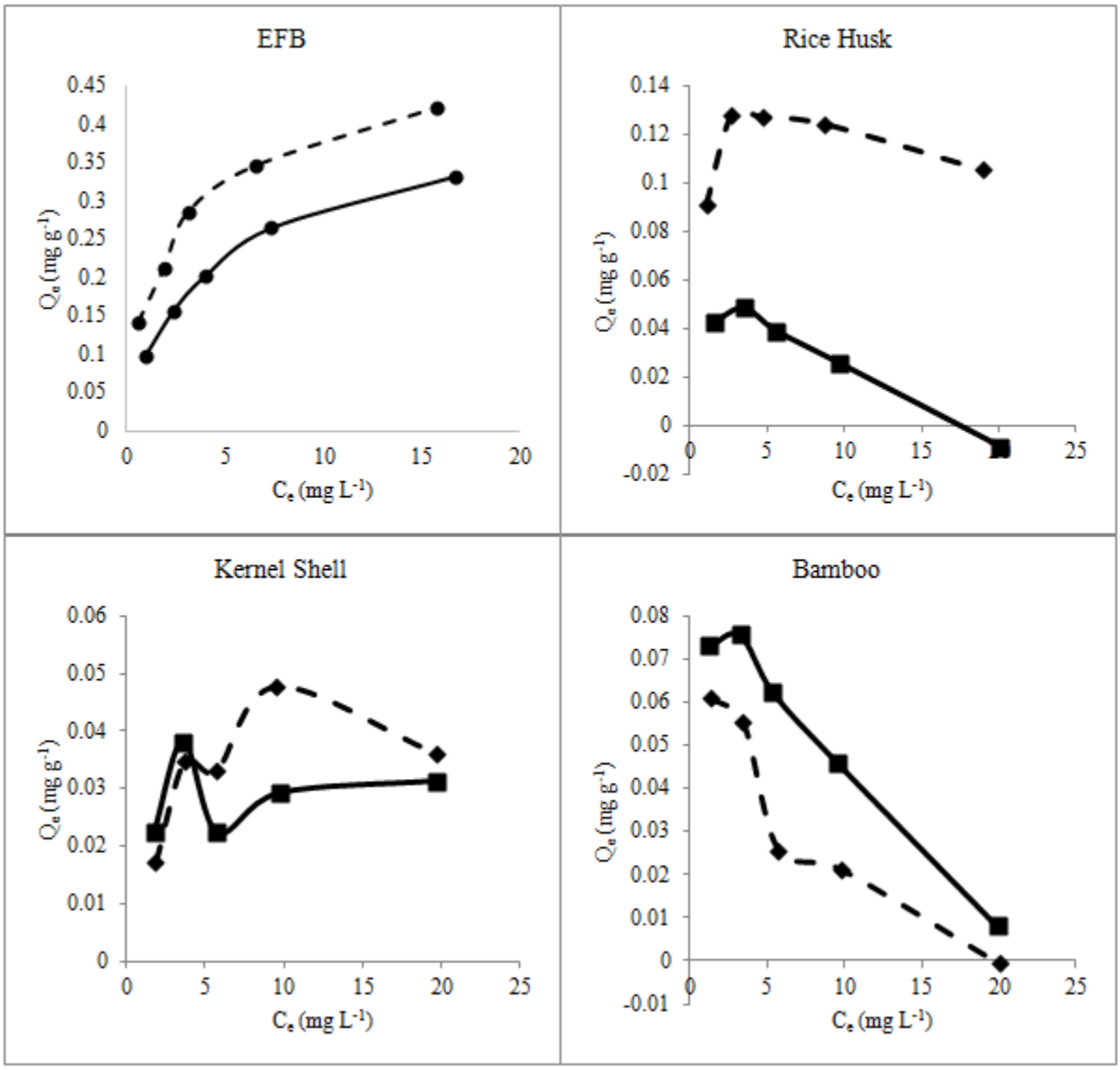

Figure 4: Sorption of Fe^{3+} in EFB, rice husk, kernel shell, and bamboo biochar. Broken lines: fine; continuous line: coarse.

ISSN: 2455-6939

Volume: 06, Issue: 02 "March-April 2020"

Table 6: Regression parameters of isotherm for expressing adsorption of Fe^{3+} to EFB, rice husk, kernel shell, and bamboo biochars at two different particle sizes.

		Freundlich			Langmuir		
		K_F	n	R^2	K_L	Q_{max}	R^2
EFB	Coarse	0.1035	2.2671	0.9818	0.2736	0.4022	0.9972
	Fine	0.1860	3.2103	0.9494	0.5056	0.4706	0.9958
RH	Coarse	0.0553	-3.7037	0.5547	-0.6860	0.0228	0.956
	Fine	0.1062	21.7865	0.1094	-1.9056	0.1048	0.9928
KRN	Coarse	0.0243	12.1951	0.1094	1.1444	0.0322	0.9762
	Fine	0.0183	3.1706	0.5646	1.1200	0.0397	0.9529
BMB	Coarse	0.0836	-1.7047	0.8365	-0.2713	0.0074	0.8757
	Fine	0.1418	-1.3665	0.6628	-0.6392	0.0183	0.9761

CONCLUSION

The BET surface area of biochars were lower in finer particle size compared to their respective coarser counterpart. Despite such unusual observation, similar situation was also reported in literature but the exact cause remains unclear. The BET surface area of biochars with coarse particle can be sorted in the order from large to small as following: bamboo > rice husk > EFB > kernel shell. Sorption affinity of ammonium on biochars were in the following order: EFB > rice husk > bamboo, while no sorption was observed on kernel shell biochar. The sorption of nitrate was well-fitted in Langmuir model with the maximum sorption capacity as following: bamboo > EFB > kernel shell > rice husk and were generally higher in fine than coarse particles. Poor sorption of phosphate was generally observed in most of the tested biochars with poor fitting in both models except in fine EFB biochar, with maximum sorption capacity of 0.2 mg g^{-1}. Unlike ammonium cation, the sorption of iron (III) was well-fitted into Langmuir model suggested the monolayer formation of sorbate onto surface active sites with relatively high maximum sorption capacity in EFB biochar while the rest were fairly low. In general, there were sorption of ammonium, nitrate and iron (III) on biochars while fairly poor for phosphate in most of the tested biochar. The sorption was generally greater in finer particle despite lower BET surface area as compared to their respective coarser particle.

ISSN: 2455-6939

Volume: 06, Issue: 02 "March-April 2020"

ACKNOWLEDGEMENTS

The authors would like to express their gratitude to Universiti Putra Malaysia (UPM) for providing the research facilities and funding under the Fundamental Research Grant Scheme (Project No.: 01-12-10-983FR).

REFERENCES

Ahmad, M., S.S. Lee, X.M. Dou, D. Mohan, J.K. Sung, J.E. Yang, and Y.S. Ok. 2012. Effects of pyrolysis temperature on soybean stover- and peanut shell-derived biochar properties and TCE adsorption in water. *Bioresource Technology*. 118: 536 – 544.

ASTM. 2007. D1762 – 84, Standard test method for chemical analysis of wood charcoal.

Bremner J.M. 1960. Determination of nitrogen in soil by the Kjeldhal method. The Journal of Agricultural Science. 55(1): 11 – 33.

Cai, T., S.Y. Park, and Y. Li. 2013. Nutrient recovery from wastewater streams by microalgae: status and prospects. *Renewable and Sustainable Energy Reviews*. 19: 360 – 369.

Campbell, C.R. and C.O. Plank. 1998. Preparation of plant tissue for laboratory analysis. Chapter 3. *In* Handbook of reference methods for plant analysis (Y.P. Kalra, ed.). Boca Raton, Fl. *CRC Press*. 37 – 49.

Demirhan, N. and F. Tuncel Elmali. 2003. Spectrophotometric determination of iron (III) with 5-nitro-6-amino-1,10-phenanthroline. *Turkish Journal of Chemistry*. 27: 315 – 321.

Ding, Y., Y.X. Liu, W.X. Wu, D.Z. Shi, M. Yang, and Z.K. Zhong. 2010. Evaluation of biochar effects on nitrogen retention and leaching in multi-layered soil columns. *Water, Air, and Soil Pollution*. 213(1): 47 – 55.

EPA. 1971. Method 352.1: Nitrogen, nitrate (colorimetric, brucine) by spectrophotometer.

Fernando, W.A., K. Xia, and C.W. Rice. 2005. Sorption and desorption of ammonium from liquid swine waste in soils. *Soil Science Society of America Journal*. 69: 1057.

Fidel R.B., D.A. Laird, and M.L. Thompson. 2013. Evaluation of modified Boehm titration methods for use with biochars. *Journal of Environmental Quality*. 42: 1771 – 1778.

Freundlich H.M.F. 1906. Over the Adsorption in Solution. *The Journal of Physical Chemistry A*. 57: 385 – 470.

Gai, X., H. Wang, J. Liu, L. Zhai, S. Liu, T. Ren, and H. Liu. 2014. Effects of feedstock and pyrolysis temperature on biochar adsorption of ammonium and nitrate. *PLoS ONE*. 9(12): e113888.

Hollister, C.C., J.J. Bisogni, and J. Lehmann. 2013. Ammonium, nitrate, and phosphate sorption to and solute leaching from biochars prepared from corn stover (*Zea mays* L.) and oak wood (*Quercus* spp.). *Journal of Environmental Quality*. 42(1): 137 – 144.

Jaafar, N.M., P.L. Clode, and L.K. Abbott. 2015. Soil microbial responses to biochar varying in particle size, surface and pore properties. *Pedosphere*. 25(5): 770 – 780.

Kameyama, K., T. Miyamoto, T. Shiono, and Y. Shinogi. 2012. Influence of sugarcane bagasse-derived biochar application on nitrate leaching in calcaric dark red soil. *Journal of Environmental Quality*. 41(4): 1131 – 1137.

Keiluweit, M., P.S. Nico, M.G. Johnson, and M. Kleber. 2010. Dynamic molecular structure of plant biomass-derived black carbon (biochar). *Environmental Science and Technology*. 44(4): 1247 – 1253.

Koroleff, F. 1976. Determination of ammonia. *In* Methods of Seawater Analysis (K. Grasshoft, ed.). *Verlag Chemie*. 126 – 133.

Laird, D., P. Fleming, B. Wang, R. Horton, and D. Karlen. 2010. Biochar impact on nutrient leaching from a Midwestern agricultural soil. *Geoderma*. 158: 436 – 442.

Langmuir, I. 1916. The Constitution and Fundamental Properties of Solids and Liquids. Part I. Solids. *Journal of the American Chemical Society*. 38: 2221 – 2295.

Mukherjee, A., A.R. Zimmerman, and W. Harris. 2011. Surface chemistry variations among a series of laboratory-produced biochars. *Geoderma*. 163: 247 – 255.

Murphy J. and J.P. Riley. 1962. A modified single solution method for the determination of phosphate in natural waters. *Analytica Chimica Acta*. 27: 31 – 36.

Qin, H., Y. Liu, L. Li, G. Pan, X. Zhang, and J. Zheng. 2012. Adsorption of cadmium in solution by biochar from household biowaste. *Journal of Ecology and Rural Environment*. 28(2): 181 – 186.

Rittmann, B.E., B. Mayer, P. Westerhoff, and M. Edwards. 2011. Capturing the lost phosphorus. *Chemosphere*. 84: 846 – 853.

Shen, Q., Y. Shen, Q. Xu, and Y. Wang. 2014. Bamboo char adsorption efficiency on soil nitrate anions. *Journal of Zhejiang A & F University*. 31(4): 541 – 546.

Sohi, S.P., E. Krull, E. Lopez-Capel, and R. Bol. 2010. A review of biochar and its use and function in soil. *Advances in Agronomy*. 105: 47 – 82.

Song, Y.H., G.L. Qiu, P. Yuan, X.Y. Cui, J.F. Peng, L. Duan, L.C. Xiang, and F. Qian. 2011. Nutrients removal and recovery from anaerobically digested swine wastewater by struvite crystallization without chemical additions. *Journal of Hazardous Materials*. 190: 140 – 149.

Sun, K., K. Ro, M. Guo, J. Novak, H. Mashayekhi, and B. Xing. 2011. Sorption of bisphenol A, 17α-ethinyl estradiol and phenanthrene on thermally and hydrothermally produced biochars. *Bioresources Technology*. 10: 5757 – 5763.

Takaya, C.A., L.A. Fletcher, S. Singh, K.U. Anyikude, and A.B. Ross. 2016. Phosphate and ammonium sorption capacity of biochar and hydrochar from different wastes. *Chemosphere*. 145: 518 – 527.

Wang, Z., H. Guo, F. Shen, G. Yang, Y. Zhang, Y. Zeng, L. Wang, H. Xiao, and S. Deng. 2015. Biochar produced from oak sawdust by lanthanum (La)-involved pyrolysis for adsorption of ammonium (NH_4^+), nitrate (NO_3^-), and phosphate (PO_4^{3-}). *Chemosphere*. 119: 646 – 653.

Yao, Y., B. Gao, M. Zhang, M. Inyang, and A.R. Zimmerman. 2012. Effect of biochar amendment on sorption and leaching of nitrate, ammonium, and phosphate in a sandy soil. *Chemosphere*. 89: 1467 – 1471.

Ye Z.L., S.H. Chen, S.M. Wang, L.F. Lin, Y.J. Yan, Z.J. Zhang, and J.S. Chen. 2010. Phosphorus recovery from synthetic swine wastewater by chemical precipitation using response surface methodology. *Journal of Hazardous Materials*. 162: 973 – 980.

Zeng, Z., S. Zhang, T. Li, F. Zhao, Z. He, H. Zhao, X. Yang, H. Wang, J. Zhao, and M.T. Rafiq. 2013. Sorption of ammonium and phosphate from aqueous solution by biochar derived fro phytoremediation plants. *Journal of Zhejiang University-SCIENCE B (Biomedicine and Biotechnology)*. 14(12): 1152 – 1161.

